

DOI: 10.1002/cmdc.201200450

Highly Ligand Efficient and Selective *N*-2-(Thioethyl)picolinamide Histone Deacetylase Inhibitors Inspired by the Natural Product Psammaphin A

Matthias G. J. Baud,^[a] Patricia Haus,^[b] Thomas Leiser,^[b] Franz-Josef Meyer-Almes,^[b] and Matthew J. Fuchter^{*[a]}

Novel picolinamide-based histone deacetylase (HDAC) inhibitors were developed, drawing inspiration from the natural product psammaphin A. We found that the HDAC potency and isoform selectivity provided by the oxime unit of psammaphin A could be reproduced by using carefully chosen heterocyclic frameworks. The resulting (hetero)aromatic amide based compounds displayed very high potency and isoform selectivity

among the HDAC family, in addition to excellent ligand efficiency relative to previously reported HDAC inhibitors. In particular, the high HDAC1 isoform selectivity provided by the chloropyridine motif represents a valuable design criterion for the development of new lead compounds and chemical probes that target HDAC1.

Introduction

The epigenetic control of chromatin organization by the covalent modification of DNA and histone proteins plays a major role in the regulation of gene expression, and consequently cell differentiation, proliferation, and survival. In recent years, it has become increasingly apparent that misregulation of epigenetic pathways participates in oncogenesis, and small-molecule inhibitors of these pathways have emerged as highly attractive targets for anticancer therapies.^[1] Selective inhibitors of epigenetic pathways should be useful not only as anticancer drugs, but also as molecular probes to study the causative relationships between specific epigenetic modifications, their biological outcomes, and how their alterations are involved in cancer.

The dynamic phenomenon of histone acetylation/deacetylation is one of the most commonly studied epigenetic events occurring on N-terminal histone tails. Acetylation/deacetylation of specific lysine residues within the histone tails is mediated by histone acetyltransferases (HATs) and histone deacetylases (HDACs), respectively.^[1] Deacetylation by HDACs causes transcriptional repression through chromatin condensation and chromatin signaling. To date, 18 human genes encoding proven or putative HDACs have been identified. HDACs fall into two categories: the zinc-dependent enzymes (classes I, II, and IV) and the NAD⁺-dependent enzymes (class III, also called sirtuins).^[1] Class I HDACs (HDAC1, 2, 3, 8) are mostly present in

the nucleus, whereas class II HDACs are tissue specific and shuttle between the cytoplasm and nucleus.^[2,3] Class II HDACs can be further subdivided into class IIa (HDAC4, 5, 7, 9) and class IIb (HDAC6, 10). HDAC11 constitutes its own class IV. Despite their name, several HDACs are able to deacetylate non-histone substrates.^[4,5] Sirtuins are structurally and mechanistically distinct enzymes.

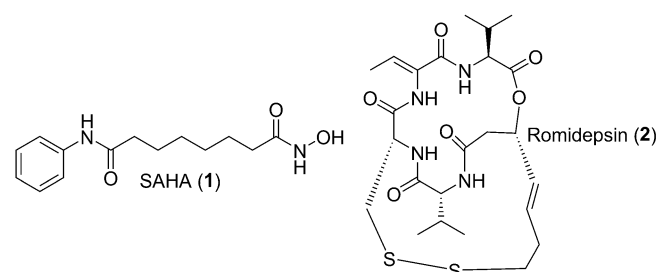


Figure 1. FDA-approved HDAC inhibitors for the treatment of CTCL.

The intensive search for HDAC inhibitors has culminated in the development and FDA approval of suberoylanilide hydroxamic acid [SAHA, 1, tradename Zolinza (Merck)] and romidepsin [2, tradename Istodax (Celgene)] for the treatment of cutaneous T-cell lymphoma (CTCL; Figure 1).^[6–8] Despite their proven success in the treatment of non-solid tumors, SAHA and romidepsin suffer from a number of drawbacks. In particular, SAHA has been shown to exhibit low specificity among zinc-dependent HDACs, whereas romidepsin only displays subclass specificity. This inherent lack of specificity is thought to be responsible for a number of adverse side effects^[9] and clearly illustrates the need for novel, selective, and metabolically stable HDAC inhibitors for anticancer therapies.

[a] M. G. J. Baud, Dr. M. J. Fuchter
Department of Chemistry
Imperial College London, London SW7 2AZ (UK)
E-mail: m.fuchter@imperial.ac.uk

[b] P. Haus, T. Leiser, Prof. Dr. F.-J. Meyer-Almes
Department of Chemical Engineering and Biotechnology
University of Applied Sciences Darmstadt
Schnittspahnstraße 12, 64287 Darmstadt (Germany)

Supporting information for this article is available on the WWW under <http://dx.doi.org/10.1002/cmdc.201200450>.

We are actively involved in the development of novel small-molecule inhibitors of epigenetic targets,^[9–13] with the ultimate goal to deliver potential drug candidates for anticancer therapy. Among the myriad of reported HDAC inhibitors, the natural product psammappin A (**3**, Figure 2),^[14] has emerged as a useful

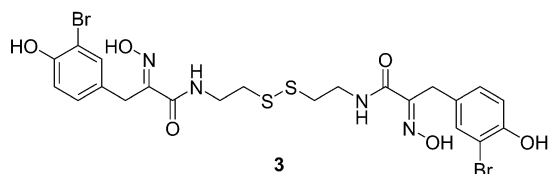


Figure 2. The natural product psammappin A.

source of inspiration for the development of new lead compounds with novel structures in the field of HDAC inhibitors.^[15,16] Psammappin A is a symmetrical, dimeric natural product, and was reported in several publications in 1987, representing the first example of a disulfide- and oxime-containing metabolite isolated from a marine sponge. The presence of the unusual α -hydroxyimino amide motif, in addition to the bromophenol functionality, confers psammappin A a fascinating structure. While it has been implicated as an inhibitor of numerous targets such as topoisomerase II,^[17] DNA gyrase,^[18] leucine aminopeptidase,^[19] farnesyl protein transferase,^[19] chitinase B,^[20] mycothiol-S-conjugate amidase,^[21] aminopeptidase N,^[22] and DNA polymerase α -primase,^[23] Crews and co-workers demonstrated psammappin A to be an extremely potent HDAC inhibitor.^[14b]

Following this study, we^[11] and others^[15] recently established a structure–activity relationship (SAR) for this natural product against a panel of HDACs. Indeed, dissection of its activity allowed us to identify the structural features responsible for its extraordinary potency and isoform selectivity (Figure 3). We unambiguously demonstrated that, similarly to romidepsin, psammappin A is a natural prodrug, displaying its strong HDAC inhibitory effect after reduction of its disulfide unit, with the thiol acting as a highly efficient zinc binding group. Additionally, we demonstrated that the oxime unit of psammappin A and related analogues is responsible for the significant HDAC1 selectivity *in vitro*. Although we previously proposed a possible

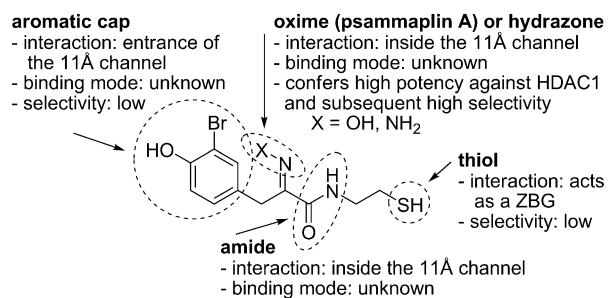


Figure 3. Structure–activity relationship of the natural product psammappin A against HDACs, adapted from Baud et al.^[11]

binding mode for psammappin A to HDAC1,^[11] we have yet to obtain unambiguous experimental evidence for this pose and therefore felt further SAR would be valuable. In terms of the oxime functionality in particular, it is still unclear whether it interacts with HDAC1 via its nitrogen, oxygen, and/or hydrogen atom. Moreover, although the oxime of psammappin A and related analogues we reported were exclusively observed with the *E* configuration (NMR), we cannot exclude the possibility of partial *in situ E-to-Z* isomerization.^[14a]

In the present study, we used the knowledge gained from our initial SAR around psammappin A in the rational design of novel and selective HDAC inhibitors, with improved drug-like properties. Indeed, although the psammappin A analogues we reported are the most potent non-peptidic HDAC1 inhibitors to date *in vitro*, the presence of metabolically unstable functional groups such as an oxime^[24] and a thiol^[25] may explain their moderate potency in cell-based assays. Here, our attention was turned exclusively toward the search for drug-like structural motifs as a replacement for the oxime.

We considered the use of functionalized aromatics and heteroaromatics to be an excellent choice for replacing the oxime of psammappin A and analogues. For example, the oxime sp^2 nitrogen atom could be mimicked by another strong σ -donor atom, such as the nitrogen atom of a pyridine unit. The H-bond donor character of a hydrazone is potentially reproduced with heterocycles such as pyrrole or pyrazole (Figure 4).

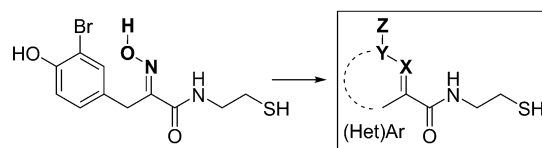


Figure 4. (Hetero)aromatics as oxime mimics for HDAC inhibition.

Results and Discussion

The synthesis of a variety of library members was straightforward and achieved through amide bond formation between an aromatic or heteroaromatic carboxylic acid derivative and cystamine **4**. A summary of structures, conditions, and yields are listed in Table 1. Detailed procedures and analytical data can be found in the Supporting Information. Carboxylic acids **5** and benzoyl chloride were all obtained from commercial sources. Ethyl 1*H*-pyrrole-3-carboxylate **5e**^[26] and methyl pyrimidine-2-carboxylate **5j**^[27] were prepared according to published procedures. Isolated product yields were generally good, except for compounds **6b**, **6e**, **6f**, **6j**, and **6l**. The low yields obtained for **6b**, **6f**, and **6l** were mostly attributed to poor solubility of both the starting materials and products. The AlMe₃-mediated amide bond formation between esters and cystamine was capricious, and afforded **6e** and **6j** in low yields. The dimers were subsequently reduced with tris(2-carboxyethyl)-phosphine (TCEP), and the corresponding thiols were assayed against class I HDAC1 and class IIb HDAC6 as described previously.^[10,11] The results are presented in Table 1.

Table 1. Synthesis of compounds **6a–m** and inhibitory potencies of the corresponding thiols **7a–m** against HDAC1 and HDAC6.

Reaction scheme: (het)Ar-X (5a-m) + cystamine 4 (H₂N-CH₂-CH₂-S-CH₂-CH₂-NH₂) reacts under conditions to form (het)Ar-CONH-CH₂-CH₂-S-CH₂-CH₂-NH₂ (6a-m). Compound 6a-m is then treated with TCEP (in situ) to yield the thiol (het)Ar-CONH-CH₂-CH₂-S-CH₂-CH₂-SH (7a-m).

Compd	Ar	Conditions ^[a]	Yield 6 [%]	IC ₅₀ [μM]		Mimic
				rHDAC1	rHDAC6	
5a		a	95	3.7	> 10	reference
5b		b, c	20	11.8	> 10	
5c		b, c	78	6.0	> 10	
5d		b, c	64	5.2	> 10	
5e		d	27	7.2	> 10	
5f		b, c	9	2.1	> 10	
5g		b, c	62	0.51	> 10	
5h		b, c	81	0.48	> 10	
5i		b, c	80	0.15	> 10	
5j		d	31	0.22	> 10	
5k		b, c	59	2.0	> 10	
5l		b, c	16	0.61	> 10	
5m		b, c	53	0.24	> 10	

[a] Conditions: a) PhC(O)Cl, cystamine **4**, Et₃N, CH₂Cl₂, 0 °C → RT, 20 h; b) ArCOOH, EDC, HOBT, CH₂Cl₂, RT, 20 min; c) cystamine **4**, Et₃N, RT, 14–40 h; d) ArCOOR, cystamine **4**, AlMe₃, CH₂Cl₂, reflux, 24 h.

Compounds bearing an H-bond acceptor in a 1,3 relationship with the amide were found to be only moderately potent, as exemplified by furan **7b** (IC₅₀: 12 μM), which was in the same range of potency as the reference compound **7a** (3.7 μM), bearing a simple phenyl ring. Varying the polarizability of the acceptor, for example with a thiophene **7c** (6.0 μM) did not have a significant effect on potency. Introduction of

the strong σ-donor pyridine **7d** again did not lead to any significant improvement. Replacing the H-bond acceptor by an H-bond donor did not have any significant influence. Indeed, pyrrole **7e** (7.2 μM) and indole **7f** (2.1 μM) still displayed potencies similar to that of the reference compound **7a** (3.7 μM).

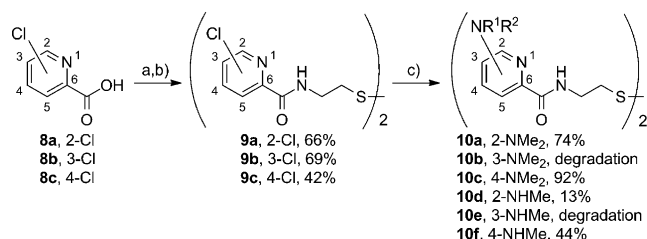
In contrast, compounds bearing a H-bond acceptor, typically a nitrogen, in a 1,2 relationship with the amide were found to be more potent than the corresponding analogues lacking this nitrogen in each case. This is clear in comparing the potencies of furan **7b** (11.8 μM) versus isoxazole **7g** (0.51 μM), pyrrole **7e** (7.2 μM) versus pyrazole **7h** (0.48 μM), unsubstituted phenyl **7a** (3.8 μM) versus *o*-pyridine **7i** (0.15 μM), and substituted phenyl **7k** (2.0 μM) versus *o*-pyridine **7m** (0.24 μM). In particular, *o*-pyridine **7i** (0.15 μM) was the best HDAC1 inhibitor and was 25-fold more potent than reference compound **7a** (3.8 μM). Moreover, six-membered ring systems were found to provide slight increases in potency relative to five-membered rings. For example, both *ortho*-pyridine **7i** (0.15 μM) and *o,o*-pyrimidine **7j** (0.22 μM) were slightly more potent than isoxazole **7g** (0.51 μM) and pyrazole **7h** (0.48 μM).

The *o*-hydroxy substituent of **7k**, designed to imitate an isomerized *Z*-configured oxime, was not found to be significantly more potent than reference compound **7a**. However, functionalization of both *ortho* positions led to a slight increase in potency, compound **7l** (0.61 μM) being three- and sixfold more potent than **7k** (2.0 μM) and **7a** (3.7 μM), respectively. As a control, SAHA (**1**) displayed an IC₅₀ value of 30 nM, in close accordance with previously reported values (27 nM).^[28]

Interestingly, and in concordance with our study on psammaplin A, the compounds from our library displayed impressive class selectivity. In particular, compounds bearing a nitro-

gen atom in the *ortho* position were highly selective against class I HDAC1 over class IIb HDAC6. This is clearly exemplified by isoxazole **7g**, pyrazole **7h**, pyridine **7i**, pyrimidine **7j**, and substituted pyridine **7m**, both displaying $IC_{50} > 10 \mu\text{M}$ against HDAC6, while being sub-micromolar inhibitors of HDAC1. Although the steric and electronic properties of an oxime/hydrazone and the heterocycles employed are different, we hypothesize these *ortho*-nitrogen containing compounds to bind to HDAC1 in a similar way as psammaplin A. This is nicely supported by the similar isoform selectivity profiles displayed by **7i** and psammaplin A (Tables 1 and 3).

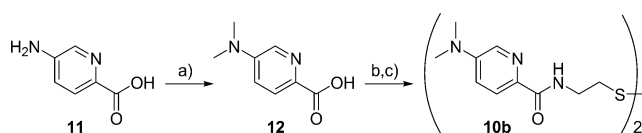
We selected pyridine **7i** for further investigation. In particular, we decided to study the influence of aromatic substitution on HDAC potency and selectivity. We hypothesized that judicious introduction of substituents on the heteroaromatic ring may have a positive influence on the potency against HDAC1. Chlorine and amine substituents were chosen as representative electron-withdrawing and electron-donating substituents, respectively. A number of chloropyridine carboxylic acids are commercially available and inexpensive. Positions 2, 3, and 4 were selected for derivatization, as vectors originating from these positions are likely to project toward the rim of the 11 Å active site HDAC channel, and therefore introduction of small substituents at these positions is most likely to be tolerated on steric grounds. The synthesis of the target compounds is illustrated in Scheme 1. EDC-mediated coupling of chloropyridine



Scheme 1. Synthesis of chloro- and amino-substituted pyridine compounds **9a–c** and **10a,c,d,f**. *Reagents and conditions:* a) EDC, HOBt, CH₂Cl₂, RT, 20 min; b) **4**, Et₃N, RT, 24 h; c) H₂NMe or HNMe₂ (40% in H₂O), THF, microwave, 160 °C.

carboxylic acids **8a–c** with cystamine **4** afforded dimers **9a–c** in moderate to good yields. Subsequent nucleophilic aromatic substitution afforded the corresponding amino derivatives **10a,c,d,f**. In each case, substitution at position 4 was found to be more efficient, due to the increased stabilization by the pyridine nitrogen atom. Substitution at positions 2 and 4 with methylamine afforded **10d** and **10f** in low yields, owing to the lower reactivity of methylamine, but also possibly due to oligomerization. Substitution with either methylamine or dimethylamine led to degradation when attempted at position 3.

Because the introduction of amine substituents at position 3 was unsuccessful by nucleophilic aromatic substitution, alternative conditions were surveyed. An Escheiwer–Clarke reaction between 5-aminopicolinic acid **11**, formic acid, and formaldehyde as previously described^[29] afforded 5-(dimethylamino)picolinic acid **12**, which was then coupled with cystamine, and



Scheme 2. Synthesis of compound **10b**. *Reagents and conditions:* a) HCOOH, HCHO, reflux, 2.5 h; b) EDC, HOBt, CH₂Cl₂, RT, 20 min; c) **4**, Et₃N, RT, 24 h, 13% over three steps.

afforded analogue **10b** in 13% yield after three steps (Scheme 2).

Dimeric compounds were reduced with TCEP as described previously,^[10,11] and the corresponding thiols were assayed against HDAC1 and HDAC6. The results are listed in Table 2. Chloropyridines **13a–c** were highly potent against HDAC1. In particular, analogue **13a** (IC_{50} : 0.021 μM) was the most potent and was sevenfold more active than the initial pyridine compound **7i** (0.15 μM). In contrast, introduction of amines at positions 2, 3, or 4 did not lead to any improvement in potency, as

Table 2. HDAC inhibition data for compounds **7i**, **13a–c**, **14a,c,d,f**, and **15**.

Compd	Ar	rHDAC1	rHDAC6
7i		0.15	> 10
13a		0.021	> 10
13b		0.087	> 10
13c		0.052	> 10
14a		0.54	> 10
14b		0.42	> 10
14c		0.29	> 10
14d		ND	> 10
14f		0.17	> 10

[a] ND: not determined.

exemplified by analogues **14a**, **14b**, **14c**, and **14f** being similarly potent or slightly less potent (0.17–0.54 μM) than **7i**. Once again, these compounds displayed high selectivity for HDAC1 with respect to HDAC6.

To further investigate the isoform selectivity of our inhibitors, the most potent compounds of each series, **7i** and **13a**, were assayed against class I HDAC2, HDAC3, and HDAC8, in addition to HDAC4 as a representative member of class IIa (Table 3). We were pleased to observe impressive selectivity for

Compd	rHDAC IC ₅₀ [μM]					
	1	2	3	8	4	6
1	0.032	0.065	0.12	4.6	20	0.13
2	0.007	0.004	0.005	0.015	0.29	0.22
3	0.001	0.006	0.009	1.3	6.3	0.36
7i	0.15	0.35	0.25	2.8	> 10	> 10
13a	0.021	0.14	0.068	4.2	> 10	> 10

HDAC1 among the other isoforms tested. Indeed, at the highest concentration tested, **7i** and **13a** were inactive against HDAC4 (IC₅₀ > 10 μM) and HDAC6 (IC₅₀ > 10 μM), used as representative members of class IIa and IIb, respectively. More interestingly, they were able to discriminate between the different isoforms within class I: **7i** and **13a** had comparatively low inhibitory potency for HDAC8. This was particularly pronounced in the case of **13a**, which was 200-fold more potent against HDAC1 (0.021 μM) than against HDAC8 (4.2 μM). Moreover, most potent compound **13a** was seven- and threefold more potent against HDAC1 than against HDAC2 (0.14 μM) and HDAC3 (0.068 μM), respectively. Although modest, this selectivity is interesting considering the very high sequence identity displayed by HDAC1, HDAC2, and HDAC3. Such a HDAC1/2/3 selectivity is currently limited to few examples. Among compounds that display such selectivity are *ortho*-aminophenyl benzamide derivatives, although low-nanomolar inhibitors based on this scaffold are rare. Herein we present potent and structurally novel HDAC inhibitors, and expand the range of structural motifs available for the selective targeting of HDAC1/2/3.

One particularly promising feature of our *N*-2-(thioethyl)picolinamide inhibitors is their low molecular weight. Indeed, using Equation (1) we calculated ligand efficiencies (LE) of select compounds from our library, along with SAHA, romidepsin, and psammaplin A (Table 4). Compound **13a** displayed an excellent LE of 0.8, higher than the parental psammaplin A, and almost twofold higher than SAHA and romidepsin.

$$\text{LE} = -1.35 \log(\text{IC}_{50})/n \quad (1)$$

for which n = number of heavy atoms

In order to provide insight into the binding mode of our ligands, we performed docking studies (Schrödinger) using the recently reported crystal structures of HDAC2 (PDB ID:

Compd	IC ₅₀ [μM]	LE
SAHA	0.030	0.53
Romidepsin	0.007	0.31
Psammaplin A	0.001	0.68
7a	3.8	0.61
7i	0.15	0.77
13a	0.021	0.80

3MAX)^[30] and HDAC3 (PDB ID: 4A69),^[31] both of which share a high sequence identity with HDAC1, notably around the active site. Similar data were obtained in both cases, and only data obtained with HDAC2 are presented. Procedures for ligands and protein preparation are described in the Experimental Section below. In our model, the *N*-(2-thioethyl)amide motif coordinates the Zn^{II} cation in a bidentate fashion (Figures 5 and 6), and the amide is involved in hydrogen bonding with Tyr308 and Gly154 (Figure 5c). A similar bidentate binding mode for the *N*-(2-thioethyl)amide motif was previously proposed by Anandan and colleagues, although experimental evidence is still lacking to date.^[32] Although the zinc binding motif is different, a similar bidentate binding mode has also been reported by Bressi et al. for an *ortho*-aminophenyl benzamide derivative.^[30]

In this context, the absence of the catalytic tyrosine residue in class IIa HDACs could explain the lack of potency of our compounds against HDAC4. Interestingly, our compounds were unable to adopt a bidentate binding mode when docked in HDAC8 (PDB ID: 1T64, data not shown).^[33] We believe this to be due to the presence of Trp154 in HDAC8 in a steric clash with the methylene unit adjacent to the sulfur atom. This tryptophan residue is absent in HDAC1, HDAC2, and HDAC3. Finally, Leu276 in HDAC2 is conserved through class I HDACs apart from HDAC8, where leucine is replaced by methionine. These differences might contribute to the observed differences in substrate and inhibitor selectivities within class I between HDACs 1, 2, 3 and HDAC8.

The role of the chloropyridine motif of **7i** and **13a–c** is unclear at this stage, however. Indeed, no specific interaction between the pyridine nitrogen and the protein was identified from our docking studies. However, the ~4 Å separating the pyridine nitrogen and His146 makes the presence of a structural water molecule bridging the ligand and the protein plausible (Figure 6a). Additional structural information and in-depth molecular dynamics will be useful for highlighting the subtle structural changes among class I HDACs responsible for the isoform selectivity of our compounds. These studies will be reported in future manuscripts.

Conclusions

In summary, our search for a molecular replacement for the oxime unit of psammaplin A led us to the discovery of novel, isoform-selective, and highly ligand efficient *N*-2-(thioethyl)picolinamide HDAC inhibitors. In addition to being easily accessi-

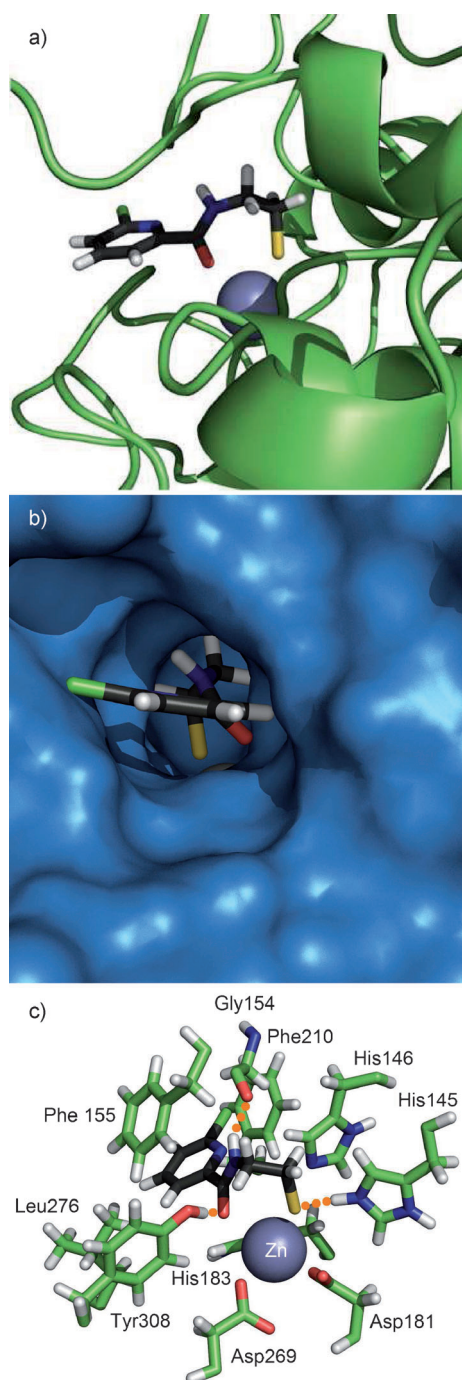


Figure 5. a) Proposed bidentate binding mode of *N*-2-(thioethyl)amide-based inhibitors within the structure of HDAC2 (PDB ID: 3MAX); b) surface representation; c) key interactions between the *N*-2-(thioethyl)amide motif and HDAC2 (front view). Grey spheres represent the Zn^{II} center.

ble synthetically, these fragment-size ligands exhibited low-nanomolar potencies and high selectivity amongst the HDAC isoforms investigated, while displaying an impressive ligand efficiency over reference compounds SAHA, romidepsin, and psammaplin A. Because selective HDAC1 inhibition has been proposed to be an effective anticancer strategy, we strongly believe that the excellent HDAC1 activity provided by the

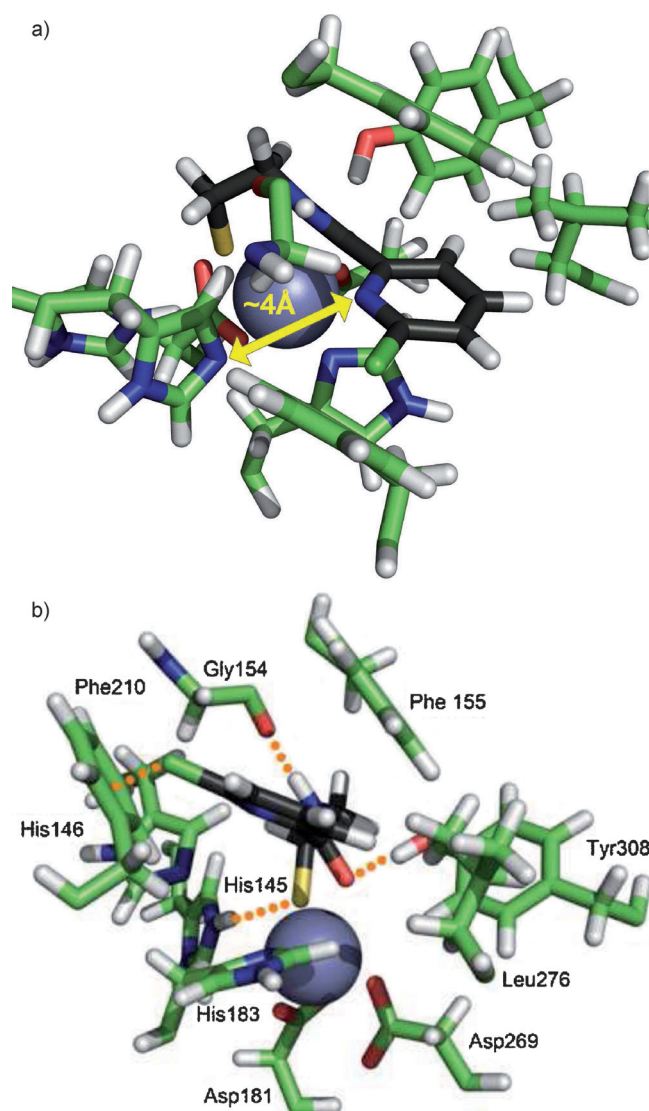


Figure 6. a) Approximately 4 Å separate His146 and the pyridine nitrogen atom of **13 a**; b) key interactions between the *N*-2-(thioethyl)amide motif of **13 a** and HDAC2 (back view); a possible π -halogen bond is also highlighted (upper left). Grey spheres represent the Zn^{II} center.

chloropyridine motif will be a valuable design criterion for the development of new lead compounds and chemical probes targeting HDAC1. Although the remaining thiol may not be an ideal functional feature owing to potential off-target effects and low metabolic stability *in vivo*,^[25] it has been shown to be tolerated in other drug candidates. This is notably exemplified with romidepsin, which has been FDA approved. Alternative zinc binding groups will be explored in subsequent studies. Moreover, we strongly believe that having a strong zinc binding group is not a prerequisite for HDAC inhibitors. Indeed, this has been recently shown by Vickers et al.,^[34] who used a cyclic tetrapeptide for surface interactions in order to compensate for the lack of interactions with Zn^{II}.

Experimental Section

Synthesis: Detailed synthetic procedures and analytical data for all compounds can be found in the Supporting Information.

HDAC assays: Thiols were obtained from their corresponding disulfides as previously reported,^[10,11] and were assayed immediately after reduction. HDAC assays were performed as previously reported.^[10,11] DMSO, Pluronic, TCEP, and trypsin (bovine pancreas) were purchased from Sigma–Aldrich, and Boc-Lys(Ac)-AMC as well as Boc-Lys(TFA)-AMC from Bachem (Switzerland). The recombinant human histone deacetylases HDAC1–4, HDAC6, and HDAC8 were obtained from BPS Bioscience (USA). All reactions were performed in black half area 96-well microplates (Greiner bio-one, Germany) according to the general procedure described by Wegener et al.^[35] with some minor modifications. The reaction buffer contains 50 mM KH₂PO₄/K₂HPO₄, 15 mM Tris-HCl pH 8, 250 mM NaCl, 0.001% (v/v) Pluronic, and 0.005% BSA. The buffer components were purchased from Merck (Germany), Roth (Germany), and Sigma–Aldrich.

A serial dilution of test compounds was pre-incubated with 7.4 nM HDAC1, 53.6 nM HDAC2, 241 nM HDAC3, 3.9 nM HDAC4, 2.8 nM HDAC6, or 23.6 nM HDAC8 for 20 min at 21 ± 1 °C in the dark. The enzyme reaction was initiated by the addition of Boc-Lys(Ac)-AMC (for HDAC1: 80 μM, HDAC2 and HDAC3: 40 μM, HDAC6: 100 μM) or Boc-Lys(TFA)-AMC (for HDAC4: 40 μM, HDAC8: 30 μM) substrate. The reaction mixture was incubated at 30 °C in the dark and stopped after 60 min by the addition of a mixture of 67 μM trypsin and 200 nM SAHA. The fluorescence of AMC serves as an indirect measure of HDAC activity. The kinetics of AMC release was measured on a PolarStar fluorescence plate reader (BMG) using an excitation wavelength of 340 nm and an emission wavelength of 460 nm. Complete cleavage of deacetylated Boc-Lys-AMC by trypsin was achieved after ~10–15 min. The fluorescence intensity of the plateau was averaged over at least 5 min and normalized with respect to percent enzyme activity. Finally, the normalized fluorescence intensities were plotted versus the concentration of test compounds and fitted to a four-parameter logistic model^[36] to calculate the IC₅₀ values.

Docking: All ligands were docked^[30] in HDAC2 (PDB ID: 3MAX)^[30] using Glide.^[37] The protein structure was prepared using the Protein Preparation Wizard^[38] from Schrödinger. His145 was protonated. Ligands were prepared (LigPrep)^[39] and docked (Glide)^[37] in their deprotonated forms (thiolate). No constraint was applied to the system. Docking poses were subjected to one round of Prime^[40] minimization, then analyzed visually with PyMOL, and distances were calculated in PyMOL.^[41]

Acknowledgements

This work was supported by the Association for International Cancer Research (08-0407).

Keywords: epigenetics · HDAC inhibitors · isoform selectivity · ligand design · psammoplanin A

[1] C. B. Yoo, P. A. Jones, *Nat. Rev. Drug Discovery* **2006**, *5*, 37–50.

[2] R. W. Johnstone, *Nat. Rev. Drug Discovery* **2002**, *1*, 287–299.

[3] W. Xu, R. Parmigiani, P. Marks, *Oncogene* **2007**, *26*, 5541–5552.

[4] S. Crabb, M. Howell, H. Rogers, M. Ishfaq, A. Yurek-George, K. Carey, B. Pickering, P. East, R. Mitter, S. Maeda, P. Johnson, P. Townsend, K. Shin-Ya, M. Yoshida, A. Ganesan, G. Packham, *Biochem. Pharmacol.* **2008**, *76*, 463–475.

- [5] T. Miller, D. Witter, S. Belvedere, *J. Med. Chem.* **2003**, *46*, 5097–5116.
- [6] P. A. Marks, R. Breslow, *Nat. Biotechnol.* **2007**, *25*, 84–90.
- [7] B. S. Mann, J. R. Johnson, M. H. Cohen, R. Justice, R. Pazdur, *Oncologist* **2007**, *12*, 1247–1252.
- [8] S. J. Whittaker, M.-F. Demierre, E. J. Kim, A. H. Rook, A. Lerner, M. Duvic, J. Scarisbrick, S. Reddy, T. Robak, J. C. Becker, A. Samtsov, W. MacCulloch, Y. H. Kim, *J. Clin. Oncol.* **2010**, *28*, 4485–4491.
- [9] F. Cherblanc, N. Chapman-Rothe, R. Brown, M. J. Fuchter, *Future Med. Chem.* **2012**, *4*, 425–446.
- [10] M. G. J. Baud, T. Leiser, F.-J. Meyer-Almes, M. J. Fuchter, *Org. Biomol. Chem.* **2011**, *9*, 659–662.
- [11] M. G. J. Baud, T. Leiser, P. Haus, S. Samlal, A. C. Wong, R. J. Wood, V. Petrucci, M. Gunaratnam, S. Hughes, L. Buluwela, F. Turlais, S. Neidle, F.-J. Meyer-Almes, A. J. P. White, M. J. Fuchter, *J. Med. Chem.* **2012**, *55*, 1731–1750.
- [12] P. Di Fruscia, K.-K. Ho, S. Laohasinnarong, M. Khonghow, S. H. B. Kroll, S. A. Islam, M. J. E. Sternberg, K. Schmidtkunz, M. Jung, E. W.-F. Lam, M. J. Fuchter, *MedChemComm* **2012**, *3*, 373–378.
- [13] B. Peck, C. Y. Chen, K. K. Ho, P. Di Fruscia, S. S. Myatt, R. C. Coombes, M. J. Fuchter, C. D. Hsiao, E. W.-F. Lam, *Mol. Cancer Ther.* **2010**, *9*, 844–855.
- [14] a) L. Arabshahi, F. J. Schmitz, *J. Org. Chem.* **1987**, *52*, 3584–3586; b) I. C. Piña, J. T. Gautschi, G. Y. S. Wang, M. L. Sanders, F. J. Schmitz, D. France, S. Cornell-Kennon, L. C. Sambucetti, S. W. Remiszewski, L. B. Perez, K. W. Bair, P. Crews, *J. Org. Chem.* **2003**, *68*, 3866–3873; c) E. Quiñoà, P. Crews, *Tetrahedron Lett.* **1987**, *28*, 3229–3232; d) A. D. Rodriguez, R. K. Akee, P. J. Scheuer, *Tetrahedron Lett.* **1987**, *28*, 4989–4992.
- [15] J. García, G. Franci, R. Pereira, R. Benedetti, A. Nebbioso, F. Rodriguez-Barrios, H. Gronemeyer, L. Altucci, A. R. de Lera, *Bioorg. Med. Chem.* **2011**, *19*, 3637–3649.
- [16] A. Nebbioso, R. Pereira, H. Khanwalkar, F. Matarese, J. Garcia-Rodriguez, M. Miceli, C. Logie, V. Kedingler, F. Ferrara, H. G. Stunnenberg, A. R. De Lera, H. Gronemeyer, L. Altucci, *Mol. Cancer Ther.* **2011**, *10*, 2394–2404.
- [17] D. Kim, I. S. Lee, J. H. Jung, C. O. Lee, S. U. Choi, *Anticancer Res.* **1999**, *19*, 4085–4090.
- [18] D. Kim, I. S. Lee, J. H. Jung, S. I. Yang, *Arch. Pharmacol. Res.* **1999**, *22*, 25–29.
- [19] J. Shin, H. S. Lee, Y. Seo, J. R. Rho, K. W. Cho, V. J. Paul, *Tetrahedron* **2000**, *56*, 9071–9077.
- [20] J. N. Tabudravu, V. G. H. Eijnsink, G. W. Gooday, M. Jaspars, D. Komander, M. Legg, B. Synstad, D. M. F. van Aalten, *Bioorg. Med. Chem.* **2002**, *10*, 1123–1128.
- [21] G. M. Nicholas, L. L. Eckman, S. Ray, R. O. Hughes, J. A. Pfefferkorn, S. Barluenga, K. C. Nicolaou, C. A. Bewley, *Bioorg. Med. Chem. Lett.* **2002**, *12*, 2487–2490.
- [22] J. S. Shim, H. S. Lee, J. Shin, H. J. Kwon, *Cancer Lett.* **2004**, *203*, 163–169.
- [23] Y. H. Jiang, E.-Y. Ahn, S. H. Ryu, D.-K. Kim, J.-S. Park, H. J. Yoon, S. Yoo, B.-J. Lee, D. S. Lee, J. H. Jung, *BMC Cancer* **2004**, *4*, 70.
- [24] a) J.-L. Boucher, M. Delaforge, D. Mansuy, *Biochemistry* **1994**, *33*, 7811–7818; b) C. T. A. Evelo, A. A. M. G. Spooren, R. A. G. Bisschops, L. G. M. Baars, J. M. Neis, *Blood Cells Mol. Dis.* **1998**, *24*, 280–295; c) P. Gross, *CRC Crit. Rev. Toxicol.* **1985**, *14*, 87–99; d) C. Kohl, C. D. Schiller, A. Gescher, P. B. Farmer, E. Bailey, *Carcinogenesis* **1992**, *13*, 1091–1094; e) N. G. M. Palmen, C. T. A. Evelo, *Arch. Toxicol.* **1998**, *72*, 270–276.
- [25] a) K. D. Held, *Radiat. Res.* **1994**, *139*, 15–23; b) T. M. Jeitner, D. A. Lawrence, *Toxicol. Sci.* **2001**, *63*, 57–64; c) R. Munday, *Free Radical Biol. Med.* **1989**, *7*, 659–673.
- [26] M. Krayner, M. Ptaszek, H.-J. Kim, K. R. Meneely, D. Fan, K. Secor, S. Lindsey, *J. Org. Chem.* **2010**, *75*, 1016–1039.
- [27] F.-T. Luo, A. Jeevanandam, *Tetrahedron Lett.* **1998**, *39*, 9455–9456.
- [28] P. Jones, S. Altamura, P. K. Chakravarty, O. Cecchetti, R. De Francesco, P. Gallinari, R. Ingenito, P. T. Meinke, A. Petrocchi, M. Rowley, R. Scarpelli, S. Serafini, C. Steinkuhler, *Bioorg. Med. Chem. Lett.* **2006**, *16*, 5948–5952.
- [29] L. W. Deady, R. A. Shanks, A. D. Campbell, S. Y. Choi, *J. Chem. Phys.* **1971**, *24*, 385–392.
- [30] J. C. Bressi, A. J. Jennings, R. Skene, Y. Wu, R. Melkus, R. De Jong, S. O’Connell, C. E. Grimshaw, M. Navre, A. R. Gangloff, *Bioorg. Med. Chem. Lett.* **2010**, *20*, 3142–3145.
- [31] P. J. Watson, L. Fairall, G. M. Santos, J. W. B. Schwabe, *Nature* **2012**, *481*, 335–340.

- [32] S.-K. Anandan, J. S. Ward, R. D. Brox, M. R. Bray, D. V. Patel, X.-X. Xiao, *Bioorg. Med. Chem. Lett.* **2005**, *15*, 1969–1972.
- [33] J. R. Somoza, R. J. Skene, B. A. Katz, C. Mol, J. D. Ho, A. J. Jennings, C. Luong, A. Arvai, J. J. Buggy, E. Chi, J. Tang, B.-C. Sang, E. Verner, R. Wynands, E. M. Leahy, D. R. Dougan, G. Snell, M. Navre, M. W. Knuth, R. V. Swanson, D. E. McRee, L. W. Tari, *Structure* **2004**, *12*, 1325–1334.
- [34] C. J. Vickers, C. A. Olsen, L. J. Leman, M. R. Ghadiri, *ACS Med. Chem. Lett.* **2012**, *3*, 505–508.
- [35] D. Wegener, F. Wirsching, D. Riester, A. Schwienhorst, *Chem. Biol.* **2003**, *10*, 61–68.
- [36] A. Volund, *Biometrics* **1978**, *34*, 357–365.
- [37] a) R. A. Friesner, J. L. Banks, R. B. Murphy, T. A. Halgren, J. J. Klicic, D. T. Mainz, M. P. Repasky, E. H. Knoll, D. E. Shaw, M. Shelley, J. K. Perry, P. Francis, P. S. Shenkin, *J. Med. Chem.* **2004**, *47*, 1739–1749; b) T. A. Halgren, R. B. Murphy, R. A. Friesner, H. S. Beard, L. L. Frye, W. T. Pollard, J. L. Banks, *J. Med. Chem.* **2004**, *47*, 1750–1759; c) R. A. Friesner, R. B. Murphy, M. P. Repasky, L. L. Frye, J. R. Greenwood, T. A. Halgren, P. C. Sanschagrin, D. T. Mainz, *J. Med. Chem.* **2006**, *49*, 6177–6196; d) Glide version 5.7, Schrödinger LLC, New York, NY (USA), **2011**.
- [38] Schrödinger Suite 2011, Schrödinger LLC, New York, NY (USA), **2011**: Epik version 2.2; Impact version 5.7; Prime version 2.3.
- [39] LigPrep version 2.5, Schrödinger LLC, New York, NY (USA), **2011**.
- [40] Prime version 3.0, Schrödinger LLC, New York, NY (USA), **2011**.
- [41] Maestro version 9.2, Schrödinger LLC, New York, NY (USA), **2011**.

Received: September 29, 2012

Revised: October 31, 2012

Published online on November 26, 2012